

## Original Research Article

# Double outlet of right ventricle: imaging spectrum on multi-slice computed tomography

Yashpal R. Rana<sup>1</sup>, Dinesh L. Patel<sup>1\*</sup>, Megha M. Sheth<sup>1</sup>, Nitisha A Jain<sup>2</sup>,  
Samir G. Patel<sup>1</sup>, Milin N. Garachh<sup>1</sup>

<sup>1</sup>Department of Radiology, U.N. Mehta Institute of Cardiology and Research Centre, Ahmedabad, Gujarat, India

<sup>2</sup>Department of Radiology, Civil Hospital, B.J. Medical College, Ahmedabad, Gujarat, India

**Received:** 16 December 2019

**Revised:** 27 December 2019

**Accepted:** 24 January 2020

### \*Correspondence:

Dr. Dinesh L. Patel,

E-mail: [drdineshpatel1965@gmail.com](mailto:drdineshpatel1965@gmail.com)

**Copyright:** © the author(s), publisher and licensee Medip Academy. This is an open-access article distributed under the terms of the Creative Commons Attribution Non-Commercial License, which permits unrestricted non-commercial use, distribution, and reproduction in any medium, provided the original work is properly cited.

## ABSTRACT

**Background:** Multi-slice computed tomography (MSCT) is the main stay of pre-operative assessment of many complex congenital heart diseases (CHD) in current clinical practice, one of them is double outlet of right ventricle (DORV). DORV is one of the conotruncal anomalies that encompasses a wide spectrum of anatomic malformations in which both the aorta and pulmonary arterial trunk arise entirely or predominantly from the morphologically right ventricle (RV). Purpose of this article is to understand spectrum of DORV and associated types of ventricular septal defect (VSD) on MSCT imaging with special emphasis of usefulness of 3-D volume rendered (VR) images in pre surgical evaluation.

**Methods:** A total of 500 paediatric patients (<18 years old), who had undergone MSCT were studied during the period 2014 to 2019 at the tertiary cardiac care centre.

**Results:** 500 patients having primary/suspicious diagnosis of DORV on echocardiography during the said period were enrolled in the study. All the patients who underwent MSCT scan, were studied in detail for: DORV spectrum, associated types of VSD and its relationship to the semilunar valves. Out of 500 total subjects, subaortic VSD was the most common type of VSD observed (53%), followed by subpulmonic VSD (22%), non-committed VSD (18%) and doubly committed VSD (7%). Associations of pulmonary stenosis, subaortic stenosis and aortic co-arctation with various types of VSDs were addressed. Associated other anomalies were also analysed.

**Conclusions:** Advances in MSCT technology has revolutionized pre-surgical diagnosis, management approach and post-operative follow-up of DORV patients. Excellent image qualities along with 3D volume rendered images help surgeon understand complex morphology of DORV variants and associated types of VSD. Significant reduction in intra and post-operative mortality in DORV patients in current era is result of MSCT technology.

**Keywords:** Double outlet of right ventricle, Multislice computed tomography, Ventricular septal defect, 3- Dimensional volume rendered technique

## INTRODUCTION

Conotruncal anomalies are congenital heart defects that result from abnormal formation and septation of the outflow tracts (conotruncus) of the heart and great vessels. DORV is a type of conotruncal anomaly which encompasses a wide spectrum of anatomic malformations that are characterized by origin of both the aorta and

pulmonary arterial trunks entirely or predominately from the morphological right ventricle (RV).<sup>1,2</sup> When an arterial valve or valves override(s) the ventricular septum through a VSD, a '50% rule' is applied.<sup>3</sup> By this rule, an overriding arterial trunk is considered as arising from the RV when more than half of the circumference of its valve belongs to the RV. As the term "DORV" describes a form of ventriculoarterial connection, it occurs with any

combination of visceratrial situs and atrioventricular connection, making it an extremely heterogeneous group. The variability of the infundibular and intracardiac morphology results in distinctively different clinical manifestations and requires comprehensive diagnostic approach and different surgical management options.

Although echocardiography is considered as an initial imaging modality of choice, it is limited in the reliable assessment because of operator dependency, a small field of view and acoustic window, poor assessment of extra-cardiac complex vascular anatomy.

Cross-sectional imaging with MSCT or magnetic resonance (MR) help overcome the limitations of conventional angiography as well such as overlap of adjacent cardiovascular structures, difficulties in simultaneously depicting the systemic and the pulmonary vascular systems, and catheter-related complications.<sup>4</sup> Radiologists should understand and become familiar with the complex morphology and physiology of DORV, as well as with various palliative and corrective surgical procedures performed in these patients. Non-invasive MSCT imaging is pivotal in the post-operative follow-up of such patients.

**METHODS**

A total of 500 subjects (<18 years old) who had undergone MSCT angiography procedure were studied during the period April 2014 to September 2019.

**Inclusion criteria**

MSCT imaging was done in all those paediatric patients in whom echocardiography revealed primary/suspicious diagnosis of DORV for further detailed evaluation and deciding surgical planning. Blood investigations like - HIV, HBsAg, Serum creatinine of all patients were mandatory.

Very small patients (<10 kg weight, < 1 month old) were first admitted and then underwent MSCT imaging for sake of pre and post procedure observation. Whenever required, sedation was done by a trained anaesthesiologist. Those who were given sedation were monitored for 4 hours. Patients who had fever or respiratory tract infection were given appropriate treatment and asked to come back for MSCT scan at a later date.

**Exclusion criteria**

Terminally sick patients or patients whose parents were not willing to consent were excluded from the study.

MSCT scan was performed on the 128 slice Somatom Definition AS+ scanner with injection of non-ionic contrast media via an intravenous line in leg (preferably) or hand. A trained paediatric anaesthetist was always present during the procedure. Contrast injection was

through a dual head pressure injector and contrast injection was followed by saline chaser to minimize the artefacts. MSCT scan parameters were as shown in Table 1. Total radiation dose varied from 5-7 mSv. Care dose radiation dose modulation technique (Siemens) was used during the procedure to minimize radiation. Steps for minimizing radiation dose are as shown in Table 2.

**Table 1: MSCT technique parameters.**

Parameter	Method
Scanner	128 slice SOMATOM Definition AS+; (Siemens Healthcare, Germany).
Contrast medium and amount	Non-ionic, 2 ml/kg Saline chaser (half that of contrast amount)
Flow rate	2 - 3 ml/sec
Scan timing	Bolus tracking, Scan triggered at 100 HU
kV	80/100
Effective mAs	40 - 100

**Table 2: Steps to minimize radiation dose.**

Measures to reduce the radiation dose
Most of the scans were performed non-ECG gated
Automatic current modulation technique
Low kVp
Justifying CT examination rigorously and eliminate inappropriate referrals.
Reduce the number of multiple phase scans, Scan only the indicated area (“child-size” the scan)
Use alternative approaches, such as MRI where appropriate
Shielding
Monitoring dose indices [ volumetric CT dose index (CTDI <sub>vol</sub> ) and Dose-length product (DLP) ]

All image data were evaluated using Syngovia software (Siemens Healthcare). Various image reformatting techniques including curved multi-planar reconstruction (c-MPR), maximum intensity projection (MIP) and 3D volume-rendering technique (VRT) are used to get all the clinically relevant information. It is important to examine source images as well apart from reconstructed images; as some information might be missed by interpreting only reconstructed images.

**RESULTS**

MSCT was found non-invasive to be 100% sensitive as well as specific for diagnosis of DORV and associated congenital anomalies.

Out of 500 total subjects, most common age group of presentation was from 1 months to 6 months-250 subjects (Table 3).

There were 45 subjects of <30 days, 115 subjects of 7 months to 1 year, 50 subjects of 1-5 years, 25 subjects of 6-10 years and 15 subjects of 10-18 years. There were 350 male and 150 female subjects (Table 4). Subaortic VSD was the most common type of VSD observed (53%), followed by subpulmonic VSD (22%), non-committed VSD (18%) and doubly committed VSD (7%) (Table 5).

**Table 3: Age wise distribution of patients.**

Age	No. of patients
<30 days	45
1-6 months	250
7 months -1 year	115
1 year-5 years	50
6-10 years	25
10-18 years	15

**Table 4: Sex wise distribution of patients.**

Gender	No. of patients
Male	350
Female	150

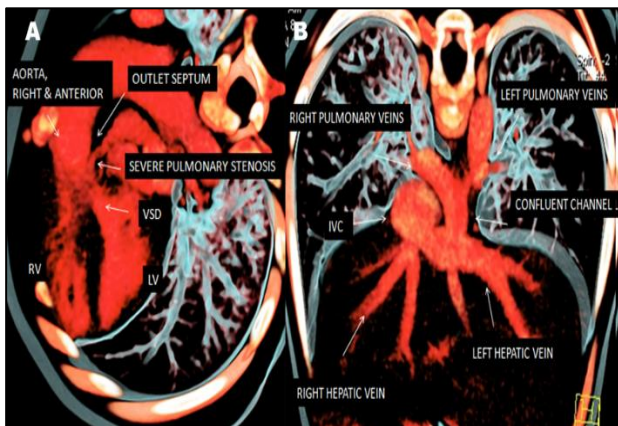


**Figure 1: DORV with Infracardiac TAPVC (A): VRT thin image showing DPRV with PS, (B): VRT thin image showing infracardiac TAPVC.**

Associations of pulmonary stenosis, subaortic stenosis and aortic co-actation with various types of VSDs are shown in (Table 6). Out of 265 subjects with subaortic VSD, 172 (64.90%) had pulmonary stenosis, 5 (1.9%) had subaortic stenosis and 12 (4.5%) had aortic co-actation. Out of 110 subjects with subpulmonic VSD, 17 (15.45%) had pulmonary stenosis, 4 (3.6%) had subaortic stenosis and 33 (30%) had aortic co-actation. Out of 35 subjects with doubly committed VSD, 21 (60%) had pulmonary stenosis, 4 (11.42%) had subaortic stenosis and 2 (5.7%) had aortic co-actation. Out of 90 subjects with non-committed VSD, 27 (30%) had pulmonary stenosis, 5 (5.5%) had subaortic stenosis and 9 (10%) had aortic co-actation.

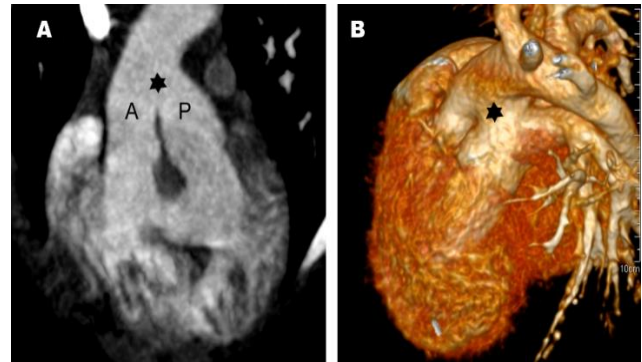


**Figure 2: DORV with type-I proximal AP (aorto-pulmonary) window. (A): Coronal oblique MIP image, (B): 3D VRT image. A= Aorta. P= Pulmonary trunk. Star mark denotes AP window.**

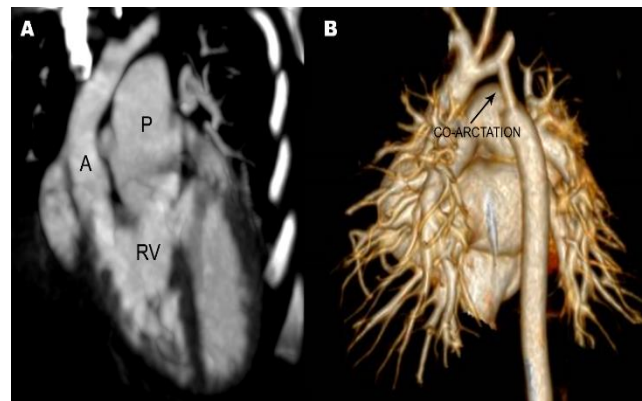


**Figure 3: DORV with juxta-ductal co-actation of aorta (A): Coronal oblique MIP image, (B): 3D VRT image. A= Aorta. P= Pulmonary trunk. RV= Right ventricle.**



**Figure 4: DORV with L-juxtaped both atrial appendages (A): Coronal oblique MIP image showing DORV, (B): Axial MPR image showing L-juxtaped both atrial appendages. A= Aorta. P= Pulmonary trunk. Star mark denotes right atrial appendage. Arrowhead mark denotes left atrial appendage.**

Associated other congenital anomalies are as follows (summarized in Table 7): 130 Endocardial cushion defects (AVCD), 96 transposition of the great arteries, 155 Right-sided aortic arch, 45 pulmonary venous anomalies. Figure

1 denotes the CT images of DORV with Infracardiac TAPVC, 1 aorto-pulmonary window.

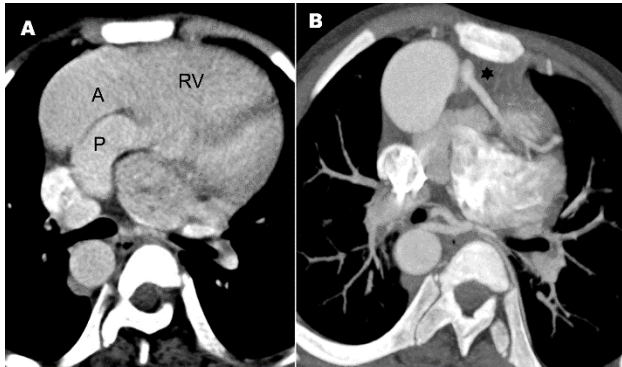


**Figure 5: DORV with coronary anomaly A): Axial oblique MIP image showing DORV, (B): Axial oblique MIP image showing coronary crossing RVOT. A= Aorta. P= Pulmonary trunk. RV= Right ventricle. Star mark denotes coronary crossing RVOT.**

Figure 2 denotes the CT images of DORV with type-I proximal AP (aorto-pulmonary) window, 56 co-arterctation.

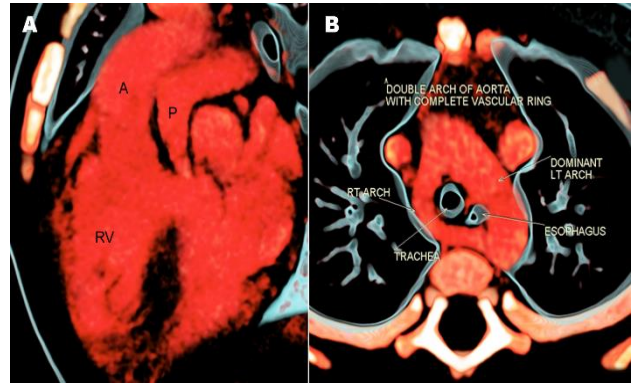


**Figure 6: DORV with double aortic arch. (A): VRT thin image showing DORV with PS, (B): VRT thin image showing double aortic arch encircling trachea and oesophagus.**

**Table 5: Types of VSD in various surgical series and its comparison with the study.**

Study	Subaortic	Sub pulmonary	Doubly committed	Non- committed
Aoki et al <sup>10</sup>	31 (42%)	27 (37%)	5 (7%)	10 (14%)
Kleinert et al <sup>11</sup>	90 (47%)	49 (25%)	5 (3%)	49 (25%)
Belli et al <sup>12</sup>	106 (59%)	37 (21%)	17 (9%)	20 (11%)
Brown et al <sup>13</sup>	57 (46%)	39 (31%)	6 (5%)	22 (18%)
Bradley et al <sup>14</sup>	156 (47%)	76 (23%)	15 (4%)	88 (26%)
Present study	265 (53%)	110 (22%)	35 (7%)	90 (18%)

**Table 6: Pulmonary and aortic outflow obstruction in the study.**

	Pulmonary stenosis	Subaortic stenosis	Obstructive lesion of the aortic arch (Aortic Co-arterctation)
Subaortic VSD (265)	172 (64.90%)	5 (1.9%)	12 (4.5%)
Subpulmonic VSD (110)	17 (15.45%)	4 (3.6%)	33 (30%)
Doubly committed VSD (35)	21 (60%)	4 (11.42%)	2 (5.7%)
Non-committed VSD (90)	27 (30%)	5 (5.5%)	9 (10%)

**Table 7: Incidence of associated other anomalies.**

Associations	No.
Endocardial cushion defects (AVCD)	130
Transposition of the great arteries	96
Right-sided aortic arch	155
Pulmonary venous anomalies	45
Aorto-pulmonary window	1
Coarctation	56
L-juxtaposed atrial appendages	76
Coronary anomalies	50
Double aortic arch	1

Figure 3 denotes the CT images of DORV with juxtaductal co-arterctation of aorta, 76 L-juxtaposed atrial appendages.

Figure 4 denotes the CT images of DORV with L-juxtaposed both atrial appendages, 50 coronary anomalies.

Figure 5 denotes the CT images of DORV with coronary anomaly and 1 double aortic arch.

Figure 6 denotes the CT images of DORV with double aortic arch.

**DISCUSSION**

DORV results from an error in formation of the conotruncus, which is the primary outlet of the heart during embryonic development. As defined earlier, DORV encompasses a wide spectrum of anatomic malformations in which both the aorta and pulmonary artery arise entirely or predominantly from the morphologically RV. DORV is associated with chromosomal anomalies such as 22q11.2 deletion syndrome, trisomy 13, trisomy 18 and CHARGE syndrome.

The hemodynamic physiology of DORV is extremely complex, VSD is the only source of egress from the left ventricle. The complexity and clinical manifestations revolve around factors like: the relation of the VSD to the arterial valves, size of the VSD and the presence or absence of aortic or pulmonary outflow tract obstruction.

The most common mode of presentation is cyanosis. Tachypnea or difficulty in breathing, poor feeding, slow weight gain and recurrent respiratory tract infections are also common.

DORV is classified into sub-types, based on the relationship of the VSD (subaortic, doubly committed, subpulmonary or non-committed) with the great arteries<sup>5</sup>. When the VSD is under the aorta, it is called as subaortic VSD. When the VSD is under the pulmonary artery, it is called as subpulmonic VSD<sup>6</sup>. When the VSD is under both of the great arteries, it is called as doubly committed and when the VSD is not near the aorta or the pulmonary artery it is called as non-committed or remote VSD. Schematic diagrams depicting various types of VSD in DORV is shown in Figure 7.

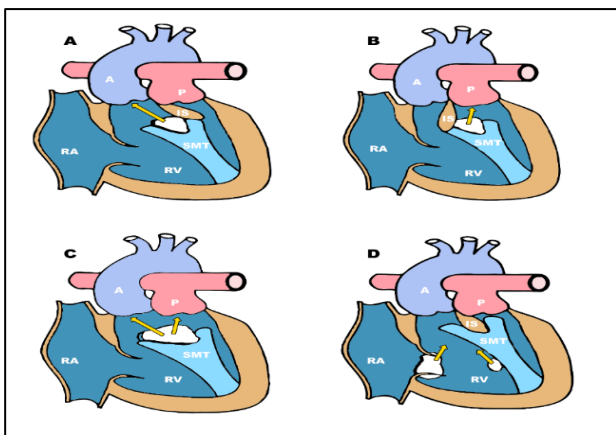


**Figure 7: Various types of VSD (A): Subaortic VSD, (B): Subpulmonic VSD, (C): Doubly committed VSD, (D) Non-committed VSD. A= Aorta. P= Pulmonary trunk. RA= Right Atrium. RV= Right ventricle. SMT= Septo-Marginal Trabeculae. IS= Infundibular Septum.**

Common variants of DORV include: A) Tetralogy of Fallot (TOF)-like variant. Figure 8 denotes the CT images

of TOF-like variant - DORV with subaortic VSD and PS. B) Transposition of great arteries (TGA)-like variant (Taussig-Bing anomaly).



**Figure 8: TOF-like variant - DORV with subaortic VSD and PS. VRT thin images showing (A): subaortic VSD, (B): pulmonary stenosis, (C) > 50% aortic override.**

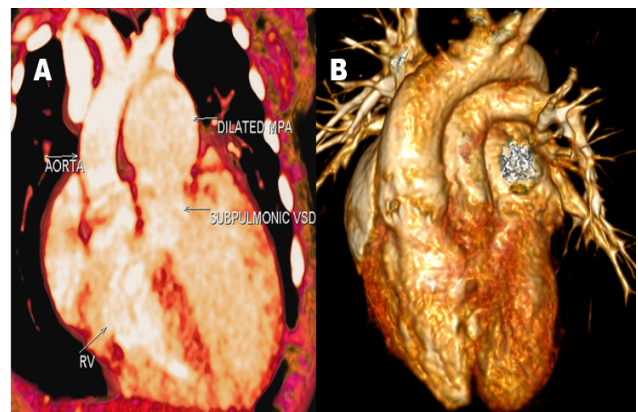


**Figure 9: TGA -like variant – DORV with a subpulmonic VSD (Taussig-Bing anomaly). (A): VRT thin image, (B): 3D VRT image showing DORV with a subpulmonic VSD.**

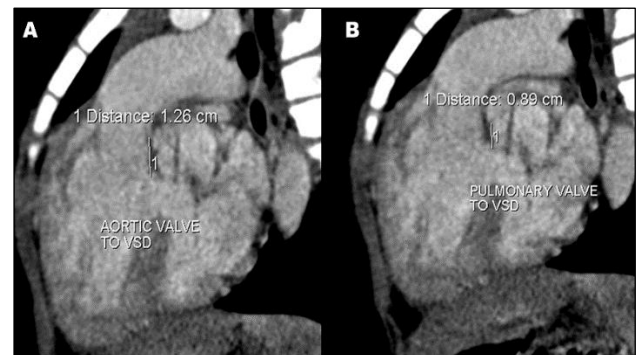


**Figure 10: DORV with Subpulmonic VSD and PS. Coronal oblique images showing (A): aortic annulus to upper border of VSD distance, (B): pulmonary annulus to upper border of VSD distance.**

Figure 9 denotes the CT images of TGA -like variant - DORV with a subpulmonic VSD (Taussig-Bing anomaly), Figure 10 denotes the CT images of DORV with subpulmonic VSD and PS and Figure 11 denotes the CT images of DORV with subpulmonic and non-committed mid Muscular VSDs. C). Variant resembling VSD. Figure 12 denotes the CT images of variant resembling VSD with subaortic VSD but without pulmonary stenosis and D) Variant resembling a univentricular heart. Figure 13 denotes the CT images of DORV variant with univentricular morphology.

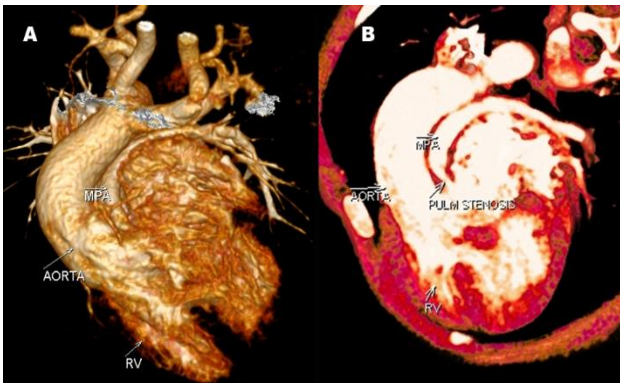


**Figure 11: DORV with subpulmonic and non-committed mid Muscular VSDs. (A): 3D VRT, (B): VRT thin image.**

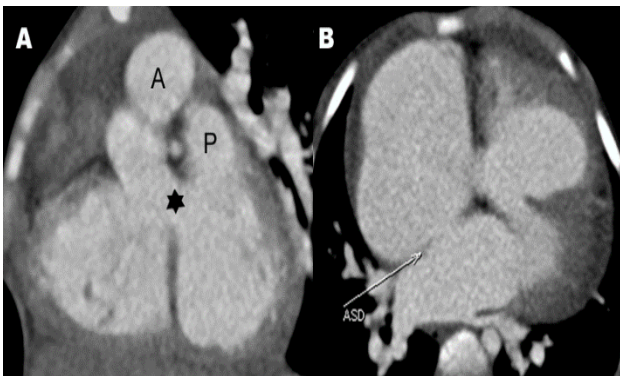


**Figure 12: Variant resembling VSD - DORV with subaortic VSD but without pulmonary stenosis. (A): Coronal oblique MPR image, (B): Axial oblique MPR image. A= Aorta. P = Pulmonary trunk. Star mark denotes VSD.**

Less frequent variants of DORV include: A) DORV with subaortic VSD, aorta left to pulmonary trunk with PS. Figure 14 denotes the CT images of DORV with subaortic VSD, aorta left to pulmonary trunk with PS. B). DORV with non-committed VSD. Figure 15 denotes the CT images of DORV with discordant atrioventricular connection and non-committed VSD. C) DORV with discordant atrioventricular connection. Figure 16 denotes the CT images of DORV with discordant atrioventricular connection. D) DORV with ambiguous atrioventricular connection. Figure 17 denotes the CT images of DORV

with situs inversus and E) DORV with mirror image atrial arrangement. Figure 18 denotes the CT images of DORV with complete AVCD, TAPVC, and right isomerism. All above mentioned different variants of DORV are summarized in Table 8.

Associated other cardiac anomalies commonly observed are endocardial cushion defects or atrio-ventricular canal defects (AVCD), coarctation of the aorta, transposition of great arteries, abnormal pulmonary venous drainage, right side aortic arch and mitral valve problems. Extracardiac anomalies, such as heterotaxy (polysplenia, asplenia, situs ambiguus) and intestinal malrotation, are frequent.

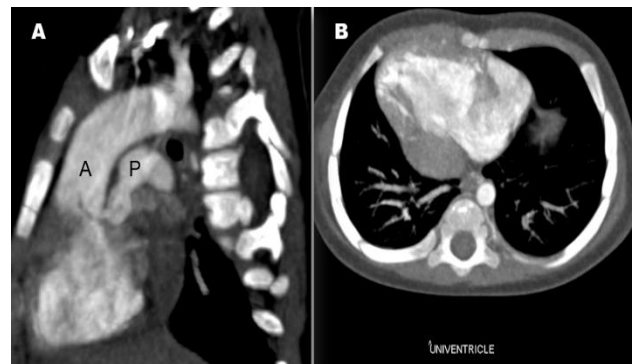


**Figure 13: DORV variant with univentricular morphology. (A): Sagittal oblique MIP image, (B): Axial oblique MPR image. A= Aorta. P = Pulmonary trunk.**

**Table 8: Variants of DORV.**

Common variants
(a) Tetralogy of Fallot (TOF)-like variant consisting of DORV with a subaortic VSD and pulmonary stenosis (PS)
(b) Transposition of great arteries (TGA)-like variant consisting of DORV with a subpulmonic VSD (Taussig-Bing anomaly)
(c) A variant resembling VSD, consisting of DORV with a subaortic VSD but without PS
(d) A variant resembling a univentricular heart
Less frequent variants
(a) DORV with subaortic VSD, Aorta left to pulmonary trunk with PS
(b) DORV with doubly committed VSD
(c) DORV with non-committed VSD
(d) DORV with discordant atrioventricular connection
(e) DORV with ambiguous atrioventricular connection
(f) DORV with mirror image atrial arrangement with any of the above combination

MSCT data set allows evaluation of the aorta, pulmonary artery and veins, cardiac chambers and ventriculoarterial connection, relationship between the upper lobe bronchi and pulmonary arteries, coronary artery, valves, systemic veins and visceral situs with a step-by-step approach.

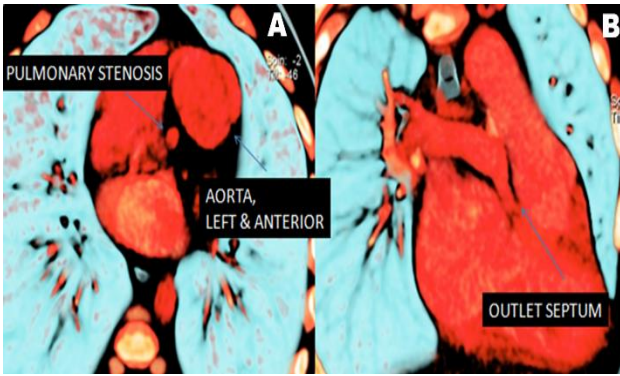


**Figure 14: DORV with subaortic VSD, Aorta left to pulmonary trunk with PS. (A): VRT thin image showing aorta left to pulmonary trunk, (B): VRT thin image showing PS and outlet septum.**

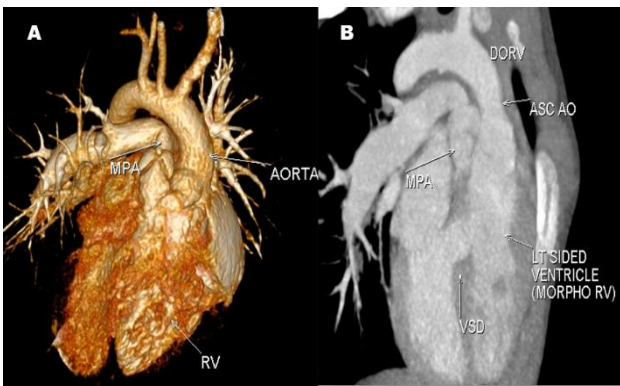


**Figure 15: DORV with discordant atrioventricular connection (Aorta left to pulmonary trunk) and non-committed VSD. (A): 3D VRT image, (B): Coronal oblique MIP image.**

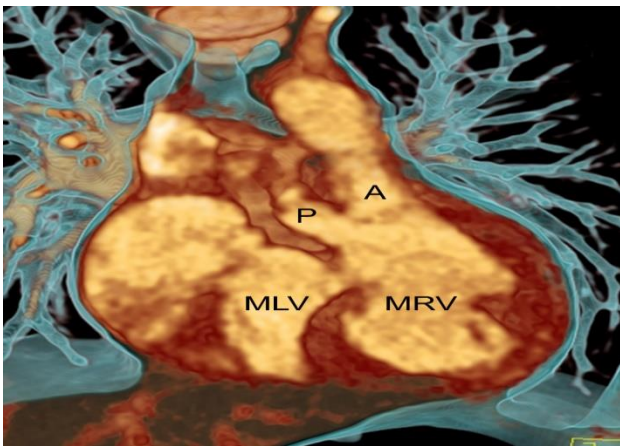


**Figure 16: Coronal oblique VRT thin image showing DORV with discordant atrioventricular connection (Aorta left to pulmonary trunk). A= Aorta. P= Pulmonary trunk. MRV= Morphological Right Ventricle. MLV= Morphological Left Ventricle.**

Preoperative MSCT with 3D Volume Rendered imaging in DORV accurately depicts type of VSD and its relationship to

the semilunar valves, size of the VSD in relation to the diameter of the pulmonary artery and aorta, distance between the VSD and aortic valve, distance between the VSD and pulmonary valve.<sup>7</sup> The morphologic structure and patency of the outflow tracts and presence and severity of subpulmonic obstruction can be well demonstrated on MSCT.<sup>8</sup> Any coexistent anomalies and the state of the extra cardiac vascular anatomy can also be evaluated on MSCT. 3D printed heart models with contrast enhanced CT/MRI in recent era is revolutionizing surgical outcome.<sup>9</sup>

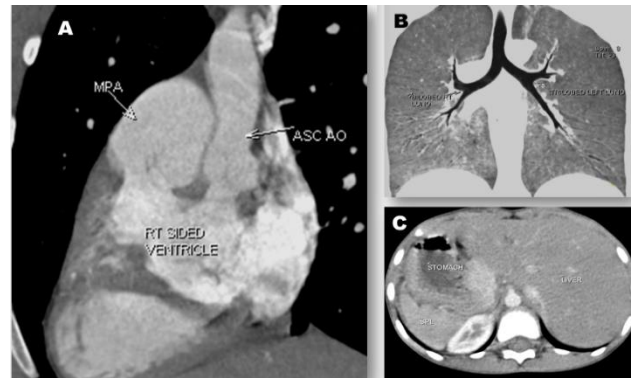


**Figure 17: DORV with situs inversus (A): Coronal oblique MIP image showing DORV, (B): Coronal MinIP image showing inverted bronchial branching pattern, (C) Axial MPR image showing spleen and stomach on right side while liver on left side.**

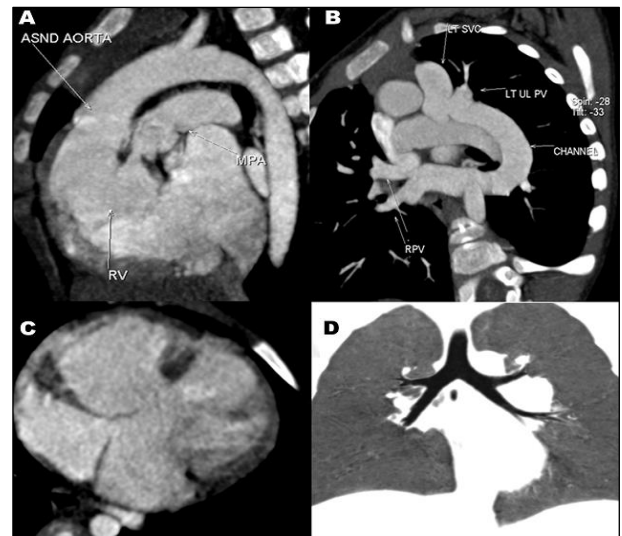


**Figure 18: DORV with complete AVCD, TAPVC, and Right isomerism (A): Coronal oblique MIP image showing DORV, (B): Coronal oblique MIP image showing supracardiac TAPVS, (C) Axial MPR image showing complete AVCD- atrio-ventricular canal defect, (D) Coronal MinIP image showing bilateral eparterial bronchi.**

Aoki et al, Kleinert et al, Belli et al, Brown et al and Bradley et al, all reported subaortic VSD as the most common type of VSD, followed by subpulmonic VSD,

non-committed VSD and doubly committed VSD. Subaortic VSD was the most common type of VSD we observed (53%), followed by subpulmonic VSD (22%), non-committed VSD (18%) and doubly committed VSD (7%). Findings of our study with respect to various types of VSDs were consistent with different studies as mentioned in Table 5.<sup>10-14</sup> MSCT has proved to be an invaluable diagnostic and decision-making tool as a compliment to echocardiography and increasingly as a substitute for invasive angiography in the management of DORV. Despite the great capabilities of MR imaging for anatomic and functional assessment of the heart, it is time-consuming and may require a lengthy period of patient sedation; hence its use in paediatric subjects, seriously ill or uncooperative patients is often limited. On the other hand MSCT offers the advantages of short acquisition times and widespread availability.

**Table 9: Management strategies based on variant of DORV.**

Type	Management
VSD type	VSD closure within first 6 months
TOF type	VSD closure with relief of pulmonary obstruction in age of 4 to 12 months
TGA type	Early corrective surgery with arterial switch, VSD closure. Alternatively, Rastelli procedure - Baffling of the LV to both arterial valves and placement of a conduit from RV to Pulmonary trunk.

The ideal surgical repair is biventricular repair by connecting the morphologically left ventricle (LV) to the aorta and the morphologically RV to the pulmonary artery, that leaves the patient with functioning right and left ventricles. The orientation of the VSD is critical for selecting the appropriate surgical approach to avoid obstructing a newly created subaortic or subpulmonary outflow channel. Various common surgical strategies depending on DORV variant, are as shown in Table 9.

## CONCLUSION

Advances in MSCT technology has revolutionized pre-surgical diagnosis, management approach and post-operative follow-up of patients with congenital heart diseases. MSCT with 3D CT imaging accurately simplifies understanding of complex morphology of DORV variants and associated types of VSDs. MSCT helps guiding the surgical approach by allowing direct evaluation of inside of cardiac chambers for RVOT, great arterial root and VSD relationships. Significant reduction in intra and post-operative mortality in DORV patients in current era is result of MSCT technology.

*Funding: No funding sources*

*Conflict of interest: None declared*

*Ethical approval: Not required*

## REFERENCES

- Walters HL, Mavroudis C, Tchervenkov CI, Jacobs JP, Lacour GF, Jacobs ML. Congenital heart surgery nomenclature and database project: double outlet right ventricle. *Ann Thorac Surg.* 2000;69:249-63.
- Lev M, Bharati S, Meng L, Liberthson RR, Paul MH, Idriss F. A concept of double outlet right ventricle. *J Thorac Cardiovasc Surg.* 1972;64:271-81.
- Wilcox BR, Ho SY, Macartney FJ, Becker AE, Gerlis LM, Anderson RH. Surgical anatomy of double outlet right ventricle with situs solitus and atrioventricular concordance. *J Thorac Cardiovasc Surg.* 1981;92:405-17.
- Sebastian L, Erwin O, Lars H. Pre and postoperative evaluation of congenital heart disease in children and adults with 64-section CT. *Radiograph.* 2007;27:3-6.
- Van PR, Geva T, Kreutzer J. Ventricular septal defects: how shall we describe, name, and classify them? *J Am Coll Cardiol.* 1989;14:1298-9.
- Stellin C, Zuberbuhler JA, Anderson RH, Siewers RD. The surgical anatomy of the Taussig-Bing malformation. *J Thorac Cardiovasc Surg.* 1987;93:560-9.
- Chen SJ, Lin MT, Liu KL, Chang CI, Chen HY. Usefulness of 3D reconstructed computed tomography imaging for double outlet right ventricle. *J Formos Med Association.* 2008;107(5):371-80.
- Shi K, Yang ZG, Chen J, Zhang G, Xu HY. Assessment of double outlet right ventricle associated with multiple malformations in pediatric patients using retrospective ECG-gated dual-source computed tomography. *Plos One.* 2015;10(6):0130987.
- Yoo SJ, Thabit O, Lee W. Double outlet right ventricle in your hands, 12 case series. *Fronti Pedia.* 2018;5:1-6.
- Aoki M, Forbess JM, Jonas RA, Mayer RE, Castaneda AR. Results of biventricular repair for double outlet right ventricle. *Thorac Cardiovasc Surg.* 1984;107:338-50.
- Kleinert S, Sano T, Weintraub RG, Karl TR, Wilkinson JL. Anatomic features and surgical strategies in double outlet right ventricle. *Circulation.* 1997;96:1233-9.
- Belli E, Serraf A, Lacour GF, Inamo J, Houyet L, Bruniaux J, et al. Surgical treatment of subaortic stenosis after biventricular repair of double outlet right ventricle. *J Thorac Cardiovasc Surg.* 1996;122:1570-80.
- Brown JW, Ruzmetov M, Okada Y, Vijay P, Turrentine MW. Surgical results in patients with double outlet right ventricle: a 20 year experience. *Ann Thorac Surg.* 2001;72:630-5.
- Bradley T, Karamlou T, Kulik A, Mitrovic B, Vigneswara T, Jaffer S, et al. Determinants of repair type, reintervention, and mortality in 393 children with double outlet right ventricle. *J Thorac Cardiovasc Surg.* 2007;134:969-73.

**Cite this article as:** Rana YR, Patel DL, Sheth MM, Jain NA, Patel SG, Garachh MN. Double outlet of right ventricle: imaging spectrum on multi-slice computed tomography. *Int J Res Med Sci* 2020;8:946-53.